INTEGRAL CHARACTERISTICS AND DOUBLE SUPPLY FREQUENCY PRESSURE PULSATIONS IN ELECTROMAGNETIC PUMPS WITH SINGLE-STAGE LINEAR CURRENT LOAD GRADING

A.P. Ogorodnikov[1], *I.R. Kirillov*[1], *G.V. Preslitsky*[1], *H. Araseki*[2]

[1] *D.V. Efremov Scientific Research Institute of Electrophysical Apparatus, 196641 St.-Petersburg, Russia, (ogorodap@sintez.niiefa.spb.su)*

[2] *Central Research Institute of Electric Power Industry, Abiko Research Laboratory, 1646 Abiko, Abiko-shi, Chiba-ken, 270-11, Japan*

Introduction. It is known [1, 2, 3] that the longitudinal end effect in linear induction pumps results in the developed pressure decrease and in arising of pressure pulsation with double frequency of the power supply source. Different methods of linear current load reduction at the inductor ends (grading), in particular, according to the linear law over one or two pole pitches [4, 5] are used to improve pumps characteristics and to decrease the double supply frequency pressure pulsation (DSF).

The DSF pressure pulsation and integral characteristics of the pumps with single-stage grading of linear current load at the inductor ends over the pole pitch length are analysed in this paper.

1. Main assumptions and the model scheme. The model scheme is shown in Fig. 1.

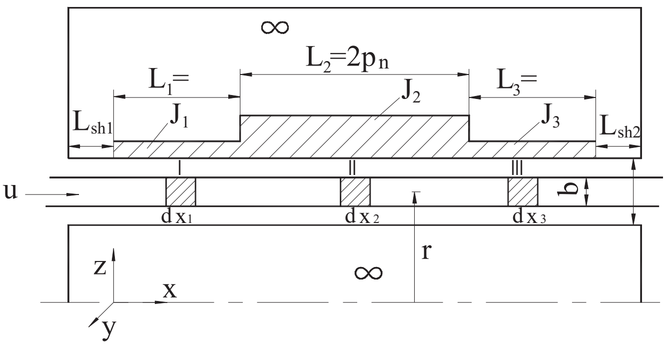

Fig. 1. Scheme of the model.

We take the following assumptions:

- the magnetic cores have the magnetic permeability $\mu = \infty$ and the finite length;
- the non-magnetic gap δ is constant over the inductor length and small $\delta \ll \tau$, $\delta \ll r$ $r \gg \tau$, where τ is the pole pitch, r is the mean radius of the duct;
- the winding has half a number of turns at the inductor ends over the pole pitch τ;
- the duct height b is constant and small, the liquid metal is moving in the direction of the x-axis at a constant velocity;
- the inductor shunting parts $L_{\rm sh1} = L_{\rm sh2} = L_{\rm sh}$ are introduced to take account of the magnetic field shunting effect.

These assumptions enable to solve the problem as a 1-D one with all electromagnetic field components depending only on x.

The linear current density (load) at the inductor surface is expressed in the following way:

$$J_1 = 0.5A_m \cos(\omega t - \alpha x_1) \qquad 0 \le x_1 \le \tau,$$
$$J_2 = -A_m \cos(\omega t - \alpha x_2) \qquad 0 \le x_2 \le 2p_n\tau,$$
$$J_3 = -0.5A_m \cos(\omega t - \alpha x_3) \qquad 0 \le x_3 \le \tau,$$

Then, using the Ampere law and the principle of magnetic flux continuity, we obtain, similarly to [2], the following equations for the induction of the applied magnetic field in the non-magnetic gap:

$$B_{\mathrm{sh1}} = B_{\mathrm{sh2}} = -B_m k_r \sin\omega t; \qquad B_{\mathrm{I}} = (0.5 - k_r)B_m \sin\omega t - 0.5B_m \sin(\omega t - \alpha x_1);$$
$$B_{\mathrm{II}} = k_r B_m \sin\omega t + B_m \sin(\omega t - \alpha x_2); B_{\mathrm{III}} = (0.5 - k_r)B_m \sin\omega t - 0.5B_m \sin(\omega t - \alpha x_3),$$

where x_1, x_2, x_3 are the coordinates counted from each zone origin, $A_m = \sqrt{2}Ak_{\mathrm{w}}$ is the amplitude of linear current load, $A = mIw/p_n\tau$ is the linear current load, m denotes a number of phases, I is the effective value of the current in phase, $B_m = \mu_0 A_m/\alpha\delta$ is the amplitude value of induction, k_{w} is the winding coefficient, $l = 2p_n\tau + 2\tau + 2L_{\mathrm{III}}$ is the total length of the inductor, $k_r = \tau/l$, $\alpha = \pi/\tau$, $\omega = 2\pi f$ is the angular frequency.

2. Solution method and results' analysis. If we assume that the magnetic field from currents in the liquid metal and in the duct walls is much less than the applied magnetic field ($\mathrm{Rm_e} s \ll 1$), then the resulting magnetic field will be equal to the applied one. Here $\mathrm{Rm_e}$ is an equivalent Reynolds magnetic number, s denotes slip. The electromagnetic pressure in each zone and the total electromagnetic pressure developed by the pump may be found similarly to [2] as:

$$p_{em}/p_0 - p_{em1} + p_{2fs}\sin(2\omega t) + p_{2fc}\cos(2\omega t), \tag{1}$$

where

$$p_{em1} = k_r^2(s-1)(1+k_{\mathrm{sh}}) + s + \left[k_r^2(s-1) + s(0.5-k_r) + 0.25\right]/p_n \tag{2}$$

is the electromagnetic pressure component independent on time,

$$p_{2fs} = -k_r^2 k_{\mathrm{sh}}\alpha L_{\mathrm{sh}} + \pi(0.5-k_r)k_r + (0.5-k_r)\left[k_r\alpha L_{\mathrm{sh}} - \pi(0.5-k_r)\right]/p_n \tag{3}$$

is the pulsating component amplitude proportional to $\sin 2\omega t$

$$p_{2fc} = k_r^2(1-s)(1+k_{\mathrm{sh}}) + \left[0.25 + k_r(k_r-1)\right]/(1-s)p_n \tag{4}$$

is the pulsating component amplitude proportional to $\cos 2\omega t$,
$p_0 = \sigma B_m^2 V f p_n \tau$ – base pressure, $Vf = 2\tau f$ – velocity of the travelling magnetic field, $k_{\mathrm{sh}} = L_{\mathrm{sh}}/p_n\tau$ – magnetic flux shunting coefficient.

As seen from expressions (3) and (4), the amplitudes of the normalised DSF pressure pulsation components are proportional to the electric conductivity of liquid metal, to the square of magnetic field induction, to the active length of the pump, and to the coefficients k_{sh}, k_r. The component changing as $\sin 2\omega t$ is proportional also to the velocity of travelling magnetic field and does not depend on slip, while the component changing as $\cos 2\omega t$ is proportional to the liquid metal velocity.

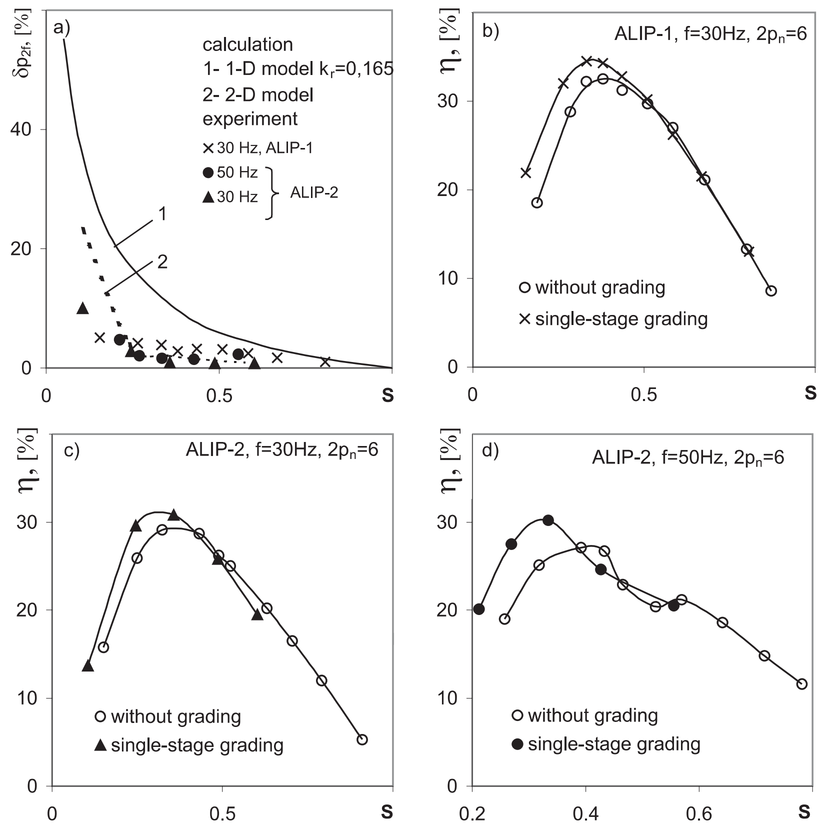

Fig. 2. Relative amplitude of the DSF pressure pulsation (*a*) and efficiency (*b*,*c*,*d*) versus slip.

Uniting pulsating components in (1) similarly to [2], we obtain the expression for relative amplitude of the DSF pressure pulsation at the pump outlet:

$$\delta p_{2f} = p_{2f}/p_{em1} = \left(p_{2fs}^2 + p_{2fc}^2\right)^{1/2}/p_{em1}\,. \tag{5}$$

Analysis of expression (5) shows that the relative amplitude of the DSF pressure pulsation depends on the coefficient k_{sh}, on the pole pairs number, on slip and on the coefficient $k_r = \tau/l$.

3. Comparison of calculated and experimental results. Two annular linear induction pumps (ALIP-1 and ALIP-2) were sodium tested at 230°C [3, 6], where one can find the pumps' main data and the measuring equipment as well. The experiments were carried out at 30 Hz for ALIP-1 and 30 and 50 Hz for ALIP-2. For ALIP-1 the tests with and without grading were carried out at the same power consumed from the network. For ALIP-2 the experiments with and without grading were carried out at the same power supply voltage: $U = 160$ V at $f = 30$ Hz and $U = 250$ V at 50 Hz. The single-stage grading was used in both cases.

The relative amplitude of the DSF pressure pulsation for both pumps versus slip s is shown in Fig. 2*a*. The experimental data are the averaged ones over five piezoelectric transducers installed at the pump inlet and outlet.

Electromagnetic pressure was found as a sum of the pump developed pressure and measured hydraulic losses obtained with the use of another pump. This figure shows also the calculated data (curve 1 for a 1-D model according to obtained expression (5) and curve 2 for a 2-D model [3]). For ALIP-1 the value of coefficient

$k_r = 0.165$ was defined experimentally according to themagnetic field induction distribution with d.c. over the inductor length. Corresponding value $L_{\rm sh} = 4.4$ mm is equal to the physically existing length of the shunting zones. For ALIP-2 $L_m = 4$ mm and $k_r = 0.165$. As seen from Fig. 2*a*, calculated and experimental data for the 1-D model fit satisfactorily at $s \geq 0.4$, but there is a discrepancy in the low slip region. The 2-D model fits well the experimental data.

The single-stage grading appears to be an effective way for decreasing the DSF pressure pulsation in the ALIP. The DSF pressure pulsations were decreased in both pumps in about 2 times comparing to the pumps without grading at slip values $s < 0.4$.

Figs. $2b, c, d$ show the experimental data pump efficiencies versus the slip at 30 and 50 Hz for single-stage grading and without grading. As seen from Figs. $2b, c, d$, the use of the single-stage grading results in the efficiency increase up to 7% at $s = 0.1$–0.5 depending on the frequency and slip.

It should be noted that the use of the single-stage grading at the same active power consumed from the network results in the applied voltage decrease by 17% and in the consumed current increase by 11-12% in comparison with the winding without grading in the studied range of slip.

4. Conclusion. The use of the single-stage grading of linear current load at the inductor ends over the pole pitch τ results in the decrease of the DSF pressure pulsation and in the pump efficiency increase in the low slip region up to 7% in comparison to the winding without grading.

REFERENCES

1. I.R. Kirillov, A.P. Ogorodnikov, V.P. Ostapenko, G.V. Preslitsky, S.I. Sidorenkov, YU.M. Tihomirov, H. Araseki. Electromagnetic pumps parameters pulsations. In *Proceedings of the Third International Conference on Transfer Phenomena in Magneto Hydro Dynamic and Electroconducting Flows* (Aussois, France, 1997), vol. 2, pp. 421–426.
2. A.P. Ogorodnikov, I.R. Kirillov, G.V. Preslitsky, H. Araseki. 1-D model for analysis of double supply frequency pressure pulsations in electromagnetic pumps. In *Proceedings of the Fifth International Pamir Conference on Fundamental and Applied MHD* (Ramatuelle, France, 2002), vol. 2, pp. 53–58.
3. H. Araseki, I.R. Kirillov, G.V. Preslitsky, A.P. Ogorodnikov. Double-supply-frequency pressure pulsation in annular linear induction pump, part I: measurement and numerical analysis. *Nuclear Engineering and Design*, vol. 195 (2000), pp. 85–100.
4. H. Araseki, I.R. Kirillov, G.V. Preslitsky, A.P. Ogorodnikov. Double-supply-frequency pressure pulsation in annular linear induction pump, part II: reduction of pulsation by linear winding grading at both stator ends. *Nuclear Engineering and Design*, vol. 200 (2000), pp. 397–406.
5. I.R. Kirillov,D.M. Obukhov, A.P. Ogorodnikov, H. Araseki. Comparison of computer codes for evaluation of double-supply frequency pulsations in linear induction pumps. *Nuclear Engineering and Design*, vol. 231 (2004), pp. 177–185.
6. H. Araseki, I.R. Kirillov, G.V. Preslitsky, A.P. Ogorodnikov. Magnetohydrodynamic instability in annular linear induction pump. Part I. Experiment and numerical analysis. *Nuclear Engineering and Design*, vol. 227 (2004), pp. 29–50.